Title Self-assembling Linear and Star Shaped Poly (e-caprolactone)/poly[(meth)acrylic acid] Block Copolymers as Carriers of Indomethacin and Quercetin

Authors Katarzyna Bury, Filip Du Prez & Dorota Neugebauer

In: Journal, Volume (Issue), pages, year. Macromol. Biosci 13(11) 1520-30, 2013.

Optional: http://onlinelibrary.wiley.com/doi/10.1002/mabi.201300179/pdf

Self-assembling linear and star shaped poly(ε-caprolactone)/poly[(meth)acrylic acid] block copolymers as carriers of indomethacin and quercetin

Katarzyna Bury[1], *Filip Du Prez*[2], *Dorota Neugebauer*[1*]

(1) Department of Physical Chemistry and Technology of Polymers, Faculty of Chemistry, Silesian University of Technology, M. Strzody 9, 44-100 Gliwice, Poland

(2) Department of Organic Chemistry, Polymer Chemistry Research Group, Faculty of Science, Ghent University, Krijgslaan 281 S4-bis, B-9000 Ghent, Belgium

* Corresponding author e-mail: dorota.neugebauer@polsl.pl

Abstract

A series of amphiphilic linear AB, BAB and star shaped $(AB)_3$ block copolymers of PCL/P(M)AA have been used for preparation of nanoparticles and drug entrapment. Both the topology of the copolymer and the type of hydrophilic segment are much influencing the critical aggregation concentration (CAC). Two different model drugs, i.e. indomethacin and quercetin, have been employed to investigate drug-copolymer interactions. The size of nanoparticles determined by DLS is less than 160 nm and increases with the amount of drug entrapped in their hydrophobic interior. Drug loading experiments with the nanoparticles based on PAA block copolymers demonstrate a higher efficiency for the star structure, whereas the PMAA star copolymer presents the lowest entrapment ability. The release properties of polymeric self-assemblies being potential candidates for new nanocarriers in drug delivery systems have been studied at room temperature and 37°C in phosphate buffer solutions with pH equal to 5 and 7.4. The kinetic profiles show a strong relation to the copolymer's topology, indicating the lowest release rates from the star based superstructures, while the PMAA particles are less stable than those containing PAA segment(s). The drug release could be controlled by changing the pH value, whereas the influence of temperature is minor.

Introduction

In recent years, the development of amphiphilic copolymers that self-assemble in aqueous solution has attracted much attention[1,2] due to the wide range of potential applications, especially as carriers in drug delivery systems (DDS). They form micelles with core-shell nanostructures, which after loading with poorly water soluble drugs, can be introduced into the human body and delivered to specific organ or target site, where the drug is expected to be released in a controlled manner. In this way, accumulation of drug is avoided leading to a reduction of toxic side effects, what is especially important in the case of application of anticancer drugs with nonspecific toxicity to normal cells.[3-7] Polymeric superstructures are characterized with a lower critical aggregation concentration (CAC) than micelles formed from low molecular weight surfactants, what is related to better stability and slower dissociation to free polymer chains.[5,8] One of the major issues in drug delivery systems is to achieve a long blood circulation half-life, which can be regulated by a particle size smaller than 200 nm. Indeed, if the micelles are recognized as foreign colloidal particles, they will be immediately removed from blood circulation through phagocytosis by the cells of the reticuloendothelial system (RES).[5,9,10]

The amphiphilic copolymers based on aliphatic biodegradable polyesters, such as poly(ε-caprolactone) (PCL) with high permeability to many drugs, can be employed as micellar carriers for controlled drug release.[3,4,11-14] The studies on micellization of PCL copolymers with hydrophilic segments of poly(ethylene oxide),[5,7,15-17] and poly(dimethylamino)ethyl methacrylate [6,18] are widely reported in literature. It was shown that the variation of the copolymer's composition provided an opportunity to modify thermodynamic and kinetic stability, degradability, or release properties of the resulting micelles/aggregates.[10,19,20] In aqueous solution, the hydrophobic character of the core enables incorporation of poorly water soluble drugs, for example indomethacine (IMC) or quercetin (QUE), into its interior by covalent or non

covalent bonding through hydrophobic interactions, making use of experimental methods such as dialysis, salting out procedure or the solvent evaporation method.[19-23]

According to the literature data[24] and Human Prescription Drug Label, IMC (2-{1-[(4-chlorophenyl)carbonyl]-5-methoxy-2-methyl-1*H*-indol-3-yl}acetic acid) is a non-steroidal, anti-inflammatory drug (NSAID) employed in the treatment of arthritis, gout, ankylosing spondylitis, bursitis, or tendinitis. This practically insoluble in water compound shows antipyretic and analgesic properties and reduces swelling and tenderness. In pharmacology, IMC is often available under the brand name Indocin. The second selected drug QUE (2-(3,4-dihydroxyphenyl)-3,5,7-trihydroxy-4H-1-benzopyran-4-one) is a flavonoid found in fruits and vegetables as well as in some seeds.[25] It presents anti-inflammatory and antioxidant properties and is known to have protective benefits when it comes to heart disease, while according to the American Cancer Society it may be effective in the prevention and treatment of cancer. Some early studies have also suggested that QUE may help to control allergies and asthma by preventing the release of histamine, which is a substance that irritates the body cells causing sneezing, itching, and other allergy type reactions.[26] However, till now QUE has not been evaluated by Food and Drug Administration for safety or efficacy.

In this article we have chosen to focus on amphiphilic linear and 3-armed star shaped block copolymers that are able to self-assemble into superstructures with a hydrophobic PCL core surrounded by a hydrophilic shell formed from poly(methacrylic acid) or poly(acrylic acid) (PMAA or PAA, respectively) with varying degree of polymerization. In this case the amphiphilicity was introduced via post-polymerization method allowing for long-term storage of copolymers with *tert*-butyl masking groups, which can be easily removed yielding weak acidic groups. Additionally, the hydrophilic P(M)AA forms a negatively charged surface, which may enhance the extent of in vitro uptake into various cell lines as well as present potential bioadhesion making them promising candidates for drug delivery to mucosal surfaces, such as respiratory, gastrointestinal and urogenitary tracts.[19] Generally, it is postulated that amphiphilic star

copolymers in comparison with their linear polymeric analogs can be organized into a more stable nanoassemblies.[24] Previously, the micelles based on diblock copolymers combining PCL and PAA were stabilized by cross-linking PAA shell, and then PCL core was selectively degraded to generate nanoscale cage-like membranes.[27] In other case the amphiphilic eight-arm star triblock copolymers with PCL-*b*-PAA-*b*-PCL arms and resorcinarene core were self-assembled into spherical micelles.[28] However, up to now the studies on PCL/P(M)AA micelles used for drug loading and release have not been reported. Our current work is aimed to compare the micellar characteristics of both drug-free and drug-loaded particles based on linear and star shaped PCL-*b*-PMAA and PCL-*b*-PAA copolymers. The systems were investigated in aqueous environment using fluorescence spectrophotometry, dynamic light scattering (DLS) and UV-Vis spectroscopy. The effect of temperature on particle size as well as the influence of pH and temperature on *in vitro* release behavior of IMC and QUE drugs from the aggregates is described. The star-shaped structure of PCLs with high-molecular weight but relatively short chains, in comparison to linear PCLs with similar molecular weight, lead to smaller hydrodynamic radius and lower crystallinity, which may affect the properties of polymer-drug system.[29] According to this, the copolymers with star structure provide enhanced stability of resulted nanoparticles, which are able to release drug at lower rate in the controlled manner. A schematic illustration of the route of research is presented in **Scheme 1**.

Scheme 1

Experimental Part

Materials. Mono-, di-, and tri-bromoester functionalized poly(ε-caprolactone)s (PCL-Br: M_n = 3100 g/mol, DP_{CL} = 25; PCL-Br_2: M_n = 2950 g/mol, DP_{CL} = 20; PCL-Br_3: M_n = 1450 g/mol, DP_{CL} = 10) were prepared according to a previously described procedure.[30] *Tert*-butyl methacrylate

(*t*BMA, Aldrich, 98 %), and *tert*-butyl acrylate (*t*BA, Alfa Aesar, 99 %) were dried over molecular sieves and stored in a freezer under nitrogen. Copper (I) bromide (CuBr, Fluka, 98 %) and copper (I) chloride (CuCl, Fluka, 97 %) were purified as reported in literature.[30] 4,4'-Dinonyl-2,2'-dipyridyl (dNdpy, Aldrich, 97 %), N,N,N',N',N''-pentamethyldiethylenetriamine (PMDETA, Aldrich, 99 %), trifluoroacetic acid (TFA, Aldrich, 99 %), indomethacin (IMC, Alfa Aesar, 98 %), and quercetin (QUE, Aldrich, 98 %) were used as received. All other chemicals were applied without purification. Distilled-deionized water was prepared with a Milli-Q Plus System (Millipore).

Synthesis of block copolymers with acidic groups ((PCL-*b*-PAA)$_n$ and (PCL-*b*-PMAA)$_n$, with n equal to 1-3): The detailed procedure of atom transfer radical polymerization (ATRP) of *t*BA or *t*BMA initiated by mono-, di- and tribromoester-functionalized PCL, which yielded linear di- and triblock copolymers as well as three-armed star shape block copolymers, was reported in our previous paper.[30] The resulting hydrophobic block copolymers were dissolved in CH_2Cl_2 (3 ml per 0.1g of copolymer), and then trifluoroacetic acid (TFA) (5 fold molar excess relative to the *tert*-butyl groups) was added. The reaction was performed for 24 h at room temperature with continuous stirring. The triblock and star-shaped copolymers were already precipitated from the reaction mixture, while diblock copolymers were precipitated in diethyl ether or heptane. Then, the amphiphilic polymers were dried under vacuum to constant mass.

Nanoparticle formation. Nanoparticles were prepared via dialysis method. The amphiphilic copolymer was dissolved in THF/H_2O (20:1 vol:vol) after what an equal amount of H_2O was added dropwise under gentle stirring and the system was stirred overnight to let micelles form. The prepared solution was dialyzed against water for 48 h to remove THF and then freeze dried.

Incorporation of drug into polymeric nanoparticles. The amphiphilic copolymer and drug (IMC, QUE) were dissolved in an organic solvent with the weight ratio of polymer:drug = 1:0.5 (or 1:1). The drug-loaded self-assemblies were prepared according to the same procedure as drug-free nanoparticles. After removal of the organic solvent, the aqueous solution was sonicated and then centrifuged to remove unloaded drug. The drug-loaded particle suspension was then frozen and lyophilized.

Characterization.

^{1}H NMR spectra were recorded in $CDCl_3$ (Eurisotop) and DMSO-d_6 (Eurisotop) on a Bruker Avance 300 at 300 MHz. Diffusion ordered nuclear magnetic resonance spectroscopy (DOSY) NMR spectra were recorded in DMSO-d_6 (Eurisotop) on a Bruker AM500 spectrometer at 500 MHz.

IR spectra were obtained on a Perkin-Elmer Spectrum 1000 FT-IR Spectrometer using Horizontal Attenuated Total Reflection (HATR).

Critical aggregation concentration (CAC) of polymeric nanoparticles was measured by fluorescence spectrophotometry (Cary Eclipse Fluorescence Spectrophotometer, Varian, Agilent Technologies) using pyrene as fluorescence probe. Excitation spectra of pyrene (λ_{em} = 390 nm) were recorded at polymer concentrations ranging from 5 x 10^{-4} to 1.0 mg/ml and constant concentration of pyrene ($3.0x10^{-4}$ M). The CAC values were estimated from the plot of the intensity ratio (I_{336}/I_{332}) from pyrene excitation spectra vs. log C (where C is concentration in mg/ml) as cross-over point at low polymer concentration.

The particle size and its distribution were measured at 25°C and/or 37°C using dynamic light scattering (DLS, Zetasizer Nano-ZS, Malvern) equipped with a He-Ne laser at fixed scattering angle (173°). Before measurement the sample (1 mg/ml) was sonicated for 0.5 h and filtered through syringe filter (pore size 0,45 μm).

The drug loaded particles were dissolved in THF (0.3 – 0.5 mg/ml) and sonicated for 10 min. The amount of entrapped drug was determined by UV-vis spectrohotometry (Specord 200PC, Analytik Jena AG) measuring absorbance at λ = 319 nm for IMC or at λ = 373 nm for QUE and using a proper calibration curve. Drug loading efficiency (DLE, %) and drug entrapment efficiency (DEE, %) were calculated from the following equations:

$$\mathrm{DLE} = \frac{\text{amount of drug in micelles}}{\text{amount of drug loaded micelles}} \cdot 100\% \quad (1)$$

$$\mathrm{DEE} = \frac{\text{amount of drug in micelles}}{\text{amount of drug fed}} \cdot 100\% \quad (2)$$

The release behavior of self-assemblies loaded with IMC or QUE were studied in different phosphate buffer solutions (PBS) with varying pH value and at different temperatures with pH equal to 7.4. Lyophilized drug-loaded polymeric nanoparticles were dissolved in PBS with pH 7.4 or 5.0 (5 mg in 2.5 ml). The solution was introduced into a dialysis membrane bag, which was placed into a glass cylinder with 50 ml of PBS and stirred at a certain temperature (37°C or room temperature). At appropriate time intervals, 2.5 ml of the buffer solution sample was taken from the release medium to determine the concentration of released drug by UV-Vis at λ = 319 nm or at λ = 373 nm for IMC or QUE, respectively. Each result is an average of three parallel measurements.

Results and discussion

Amphiphilic block copolymers

The hydrophobic block copolymers containing PCL and P*t*B(M)A segments, with linear or star shaped topologies, various molecular weights ($M_{n,GPC}$ = 8 000 – 40 000 g/mol) and narrow molecular weight distributions ($M_w/M_{n,GPC}$ = 1.15 – 1.29)[30] were converted into amphiphilic ones

by acidic hydrolysis with TFA at room temperature. The selective reaction resulted in (meth)acrylic acid units (AA and MAA) after removing *tert*-butyl groups (**Scheme 2**). Previously, these mild conditions of deprotection were employed for the hydrolysis of PtB(M)A combined with another poly(meth)acrylate segment or arranged in more complex polymer structures.[31-33]

Scheme 2

The representative HATR-FTIR spectra of triblock copolymer **III** before and after deprotection are shown in **Figure 1**. In both spectra, the stretching vibrations of the C–O bond are recognized as the band at 1100–1245 cm^{-1}, while a narrow strong band around 1700 cm^{-1} is assigned to stretching vibrations of the C=O group. In the 3100-2800 cm^{-1} region characteristic for stretching of C–H bonds, peaks originating from $\nu(CH_2)$, and $\nu(CH_3)$ are observed. After hydrolysis, the doublet at 1391 and 1366 cm^{-1} corresponding to the *tert*-butyl group is significantly diminished, whereas a broad band characteristic for O–H stretching in the acidic groups of (M)AA units appears in the region 3700–3100 cm^{-1}, which confirms effective transformation of *t*B(M)A units into (M)AA.

Figure 1

The ^1H NMR analysis also confirms the selective cleavage of *tert*-butyl groups without changes of ester linkages in PCL units. Indeed, after hydrolysis the signal at 1.45 ppm corresponding to *tert*-butyl protons is not observed, whereas the remaining multiplet signal with low intensity at 1.3-1.5 ppm, is assigned to the methylene protons in PCL segments (**Figure 2a**, **Figure S1** in Supporting Information). Additionally, the DOSY NMR was used as a powerful method based on different apparent diffusion coefficients of each chemical species in the solution, which depend on the molar mass and other hydrodynamic properties (size, shape or charge) as

well as physical properties of the surrounding environment, such as viscosity, temperature, etc.[34] The result is a 2D spectrum with chemical shift on one axis and the distribution of diffusion coefficients on the other axis. In the presented DOSY spectrum (**Figure 2b**) of sample **VI**, signals coming from only one polymer fraction are observed, which confirms that the resulting amphiphilic PCL/PMAA block copolymer is formed without any destruction of polymeric chains during the removal of *tert*-butyl groups.

Figure 2

The amphiphilic copolymers with various architectures, linear diblock AB (**I**, **II**, **V**, **VI**) and triblock BAB (**III**, **VII**), as well as three-armed star shaped $(AB)_3$ (**IV**, **VIII**), and different type of hydrophilic block, PMAA (**I-IV**) or PAA (**V-VIII**), which are presented in **Table 1**, were used for the micellization process. Additionally, differential degree of polymerization (DP_{CL} vs. $DP_{(M)AA}$), segment/arm length ($m_{(M)AA}$), and content of hydrophilic segment(s) ($F_{hydrophil}$) are expected to be responsible for the self-assembly properties of polymers in aqueous solution.

Table 1

Nanoparticle properties and drug loading

In aqueous solutions, a wide range of superstructures can be obtained through self-assembling amphiphilic block copolymers, most commonly into spherical micelles, cylindrical micelles, and vesicles,[35] whereas the micelle-like aggregates were postulated in the case of amphiphilic star block copolymers PMMA-*b*-PAA with low number of arms (f = 4)[36]. The properties of self-assemblies prepared from linear and star-shaped block copolymers PCL-*b*-P(M)AA were characterized by critical aggregation concentration (CAC) and particle size, while drug loading efficiency (DLE) and drug entrapment efficiency (DEE) were studied using drug-

loaded nanoparticles. Two different biologically active substances, IMC and QUE, were chosen as model drugs. IMC was loaded into all prepared nanoparticles, while QUE was only used in selected ones for comparative purposes.

The CAC parameter, as a minimal concentration above which both self-assembled structures and single polymer chains are present in solution, confirms aggregation but also gives information about stability of resulted nanostructures. In drug delivery application, it is important to avoid a decrease of the polymer concentration below CAC after application into the human body, because this would lead to different side effects connected with the release of high amounts of drugs unless the micelles/aggregates are kinetically stable enough. The rate of disassembly depends on the physical state of the core, which is affected by size, thermal stability and the presence of crystalline domains in the core.[19] The CAC values were measured using fluorescence spectrophotometry, where a strongly hydrophobic pyrene, known for exhibiting photochemical properties and its remarkably long life-time, was employed as a fluorescence probe. In the inset of **Figure 3**, typical fluorescence excitation spectra of pyrene in aqueous solution for copolymer **III** are presented. The spectra were recorded from 280 to 380 nm at fixed pyrene concentration for varying concentrations of amphiphilic copolymer. This shows no micelles can entrap the probe below CAC, thus the fluorescence intensity is almost non-detectable because of very low solubility of pyrene in water (2-3 μM). The maximum of the right peak is shifted from 338 to 333 nm with the decrease in polymer concentration and the intensity of fluorescence also decreases as a result of smaller amount of solubilized pyrene.

Figure 3

The plot of the intensity ratio I_{338}/I_{333} vs. logarithm of polymer concentration (logC) (**Figure 3**) for copolymer **III** was prepared on the basis of pyrene excitation spectra (at a constant

λ_{em} = 390 nm). The CAC values for all copolymers were determined as a cross point of tangents to the curve and are collected in **Table 2**. As expected, the hydrophobicity/hydrophilicity ratio is one of the major factors, which influence CAC. According to the literature, a higher hydrophobicity results in lower CAC values[37,38], what can be observed in both groups of investigated copolymers. The worth noting exception is that the CAC for sample **III** is unexpectedly lower than that of **II**, but this can be explained by significantly longer PMAA segments probably leading to a higher T_g, which in fact results in improved superstructure stability.[19] For copolymers with the same length of the hydrophobic block, the increase in the polymerization degree of poly(meth)acrylic segment(s) leads to higher CAC values and lower aggregation number of the polymeric chains. This effect can be observed when comparing copolymers **I** and **II**. Their hydrophilic fraction, which is strongly related to the polymerization degree of PMAA segment, for **I** ($F_{hydrophil.}$ = 74 mol% at DP_{MAA} = 70) is lower than in **II** ($F_{hydrophil.}$ = 78 mol% at DP_{MAA} = 89) yielding much lower CAC (0.009 vs. 0.018 mg/ml, respectively). A similar behavior is noticed for the pair of AB copolymers **V** and **VI** with polyacrylic segments (CAC = 0.006 mg/ml at $F_{hydrophob.}$ = 60 mol% vs 0.009 mg/ml at 81 mol%, respectively). The stability of micelles may also depend on copolymer structure in relation to topology and type of hydrophilic segment, i.e. polymethacrylic vs polyacrylic. The CAC values for linear diblock copolymers containing PAA are lower than for their analogs with PMAA (e.g. 0.009 mg/ml for **VI** < 0.018 mg/ml for **II**), whereas for 3-armed star shaped copolymers the correlation is exactly reversible (0.122 mg/ml for **VIII** > 0.067 mg/ml for **IV)**. In the case of linear triblock copolymers, independently on the type of hydrophilic segment, the CAC values are similar (0.013 for **VII** ≈ 0.012 for **III** mg/ml), but those copolymers also differ in the length of hydrophilic chains. Additionally, the CAC can be also controlled by the copolymer's topology, and the values are adjustable in a wide range from 0.006-0.018 mg/ml for linear chains to 0.067-0.122 mg/ml for star-shape structures. The highest

CACs presented by both PMAA and PAA star copolymers can be explained by hydrophobic interactions between star cores.

Hydrophobic drugs such as IMC or QUE, which can not be directly introduced into the human body due to their low solubility in aqueous environment (solubility of IMC in water is 0.937 mg/l, while of QUE it is 60 mg/l [39]), can be delivered by polymeric nanocarriers capable of releasing drugs in a controlled way. The drugs were loaded into the interior of the micelle according to the same procedures as those used for the preparation of drug free nanoparticles. At this stage, an important factor is the selection of the solvent that shows the ability to dissolve both drug and amphiphilic polymer. The amount of loaded drug was determined using UV-Vis spectroscopy by measuring the absorbance of IMC or QUE (at λ = 319 or 373 nm, respectively) and applying previously prepared calibration curves. The evaluated parameters of the amount of drug incorporated into the micelle (Drug Loading Efficiency, DLE) and the percentage of fed drug (Drug entrapment efficiency, DEE) are collected in **Table 2**. The ability of drug entrapment is adjusted by properties of copolymer (nature and length of core forming segments, nature of shell-domain, total molecular weight of polymer, etc.), and drug (nature, molecular volume, concentration), as well as drug-copolymer interaction.[19,26] Among the group of block copolymers containing PMAA, the values of DLE for IMC are in the range of 9 to 57 % and are increasing as follows: **IV** < **II** < **III** < **I**. Smaller values of CAC result in higher number of polymer chains to be present in the form of micelles and, as an effect, the degree of drug solubilization increases due to the larger hydrophobic volume availability for drug entrapment. In the group of PCL-*b*-PAA copolymers, DLE of IMC is much lower and does not present the above tendency, but this may be caused by the differences in the character of hydrophilic segments (PAA vs PMAA). However, the increase in hydrophilicity of copolymers with the same topology leading to higher CAC values (**I** vs. **II** and **IV** vs. **V**) results in the fact that smaller amounts of drug can be entrapped in the core (DLE = 56.8 % vs. 18.8 % or 13.4 % vs. 10.0 %, respectively). The influence of drug nature on the DLE value is evaluated by comparison of the IMC loaded micelles with that one's containing

QUE. The results show better compatibility of IMC than QUE to the investigated copolymers, yielding higher values of DLE (9.3 % vs. 3.7 % for **IV** or 15.4 % vs. 9.7 % for **VIII**, respectively). The amount of loaded drug also depends on the initial weight ratio of polymer to drug (polymer:drug = 1:0.5 or 1:1) (**Figure 4**). In the case of QUE-loaded samples, DLE is higher for nanoparticles prepared with the lower weight ratio equal to 1:0.5 instead of 1:1 (3.7 % vs. 3.2 % for **IV** or 9.7 vs. 6.9 % for **VIII**, respectively), while for IMC-loaded micelles the opposite relationship is observed (**VIII**: DLE = 15.4 % for polymer:drug = 1:0.5 vs. 20.0 % for 1:1). It is supposed that in the first example, when polymer:drug ratio exceed 1:0.5, the aggregation of unloaded QUE occurs during the micelles preparation leading to lower DLE values. This is a result of stronger hydrophobic interaction between drug molecules than that between drug and copolymer as the amount of QUE increased. Previously, similar tendency was discovered e.g. for the loading of Taxol into nanospheres composed of methoxy poly(ethylene glycol) and PCL block copolymer, where DLE increased from 4 % to 21 % as polymer:drug ratio was raised from 1:0.05 to 1:0.5 and then suddenly dropped to 9 % for polymer:drug ratio equal to 1:1.[7]

Table 2

Figure 4

The sizes of nanoparticles before and after drug loading were determined by DLS at 25 and 37 °C (**Table 3**). This parameter is responsible for particle circulation in the organism, mechanism of the entry into cells and, in turn, the kinetics and extent of cell uptake. The formed polymeric self-assemblies are characterized by monomodal size distributions by intensity, which is shown for sample **VI** in **Figure 5**. It can be observed that there are no significant changes in particle hydrodynamic diameter (d_h), indicating slightly smaller micelles at higher temperature for most of the samples when temperature is raised from 25 to 37 °C, The other observation shows that when

the length of hydrophilic segment(s) was increased (**I** vs. **II** and **V** vs. **VI**), which was related to higher CAC values, a larger nanoparticles were obtained (66.1 vs. 89.8 nm and 49.7 vs. 153.4 nm, respectively). The entrapment of drug inside the core results in the increase of hydrodynamic diameter, with the exception of sample **VI**, where smaller size of loaded nanoparticles may be explained by reduction of hydrophilic/hydrophobic repulsion of PCL, leading to the contraction of the core.[20] The polymer:drug initial weight ratio also influences the particle size, which in the case of IMC-loaded **VIII** is correlated to the formation of larger particles at higher ratio, but for QUE-loaded **IV** opposite interaction of polymer-drug is indicated due to different nature of drug. Polydispersity indices (PDI) measured by DLS for unloaded nanoparticles are in the range of 0.133 – 0.612 suggesting widely differential participation of extra associations between micelles, while drug-loaded self-assemblies are characterized with narrower size distributions up to 0.548 in case of IMC and 0.263 for the selected particles loaded with QUE.

Figure 5

Table 3

Drug release studies

The release properties were investigated using UV-Vis spectroscopy. Samples of drug loaded nanoparticles were dissolved in phosphate buffer solution (PBS) and introduced into a membrane dialysis bag. The influence of environment on the release behavior was studied in experiments performed in PBS with pH = 7.4 at room temperature and pH = 5 or 7.4 at 37 °C. These studies are particularly important due to varying pH values in different parts of the human body: stomach pH is 1 - 2, in the lower part of small intestine the pH is 7.5 ± 0.4, in ascending colon it is around 6.4 ± 0.6, while in gastrointestinal fluid it drops to 4.8.[6] The percentages of

released drug from the prepared polymeric micelles were calculated with the respect to the loading efficiencies (**Table 4**).

Table 4

The strong dependencies of drug release on topology and composition, especially within 10 h, are shown in **Figure 6a** giving the following relationships for IMC-loaded micelles based on PCL/PMAA **III** (BAB) > **II** (AB) > **IV** $(AB)_3$, and PCL/PAA **VII** (BAB) ~ **V** (AB) > **VI** (AB) > **VIII** $(AB)_3$. The highest rate of IMC release at pH = 7.4 and 37 °C is observed for the linear triblock copolymer with BAB structure (**III**), which is a reverse behavior compared to star shaped copolymer $(AB)_3$, indicating better control of drug release from micelles based on the latter one. Additionally, a higher ratio of polymer:drug causes slower release of IMC (**VIII** vs. **VIIIA**). **Figure 6b** presents the dependence of drug release rate at different pH values, where the shape of curves differs at the first stage of release (up to 10 h), but at longer time the maximum amounts of released drugs reach comparable values over 80 %. At pH = 5 the initial release of both IMC and QUE is rapid, even suggesting the occurrence of a burst effect that may be a result of the release of drug that, instead of being entrapped in the interior of hydrophobic core, is rather located in the outer hydrophilic shell or at the interface of those phases, whereas the release at pH = 7.4 is more linear and gradually increases. Moreover, the studies performed at different temperatures indicate that for copolymers with PMAA the release rate and the maximum amount of released drug is higher at 37 °C (**Figure 6c**). In the case of copolymers with PAA (**Figure 6d**) at room temperature the drug is initially released faster, but then the amount of released drug does not further increase, while at 37 °C the drug is continuously released up to 82.3 – 99.9 %. This behavior shows the strong influence of the type of hydrophilic segment, including slower release rate exhibited by PAA micelles in comparison to PMAA ones. All these results let us conclude that these micellar

systems can be well-fitted to the proper drug in order to deliver it successfully to the expected target.

Different drug release kinetic models (zero order, first order, and Higuchi) were used to describe the dissolution profiles, which are evaluated depending on the derived model parameters.[40-43] In almost all cases, the release behavior depends on the drug concentration, which means that the plots in **Figure 6** and **Figure 7a** do not follow zero-order kinetics (cumulative amount of drug released vs. time). However, a linear semilogarithmic plot of percentage of drug remaining inside the micelle vs. time in **Figure 7b**, shows good agreement with the first-order equation, yielding a correlation coefficient R^2 in the range of 0.85 – 0.99. The other interpretation of kinetics release, given by the plot of the cumulative amount of released drug against the square root of time (**Figure 7c**), is also in accordance with the Higuchi equation (R^2 = 0.91 – 0.99) that describes the systems in which the release rate is related to drug diffusion. According to the experimental data, the release process is diffusion-controlled with small deviations from linearity in **Figure 7c**, which suggest that other factors, probably such as fragmentation of PCL segment(s), may influence the drug release behavior.

Figure 6

Figure 7

Conclusions

Linear AB and BAB as well as star-shaped $(AB)_3$ hydrophobic block copolymers, containing PCL and P*t*B(M)A segments, were successfully modified into amphiphilic ones by hydrolysis of *tert*-butyl groups in mild condition with TFA at room temperature. The comparison of PMAA vs PAA block copolymers indicated that the latter ones self-assemble at lower CAC for

AB copolymers, similar for BAB, and higher values in case of AB_3 stars. The resulting micellar structures in aqueous solutions show good stability and ability to solubilize poorly water soluble drugs such as indomethacin or quercetin. The size of the investigated nanoparticles is below 160 nm and increases with the amount of loaded drug. The studies confirm that the drug loading efficiency and release behavior can be regulated by both the composition and the topology of the block copolymers. The lowest ability to entrap the drug is observed for the micelles formed by the star-shaped copolymer with PMAA segments (9 %), whereas in the series of PAA block copolymers, the star structure is the most efficient (15 – 20 %). The nanoparticles based on AB_3 star polymers exhibit slower drug release than their linear block analogs (45 % vs. 60 – 90 % with PMAA and 25 % vs. 55 – 60 % with PAA within 10 hours), and PAA-based block copolymers are more efficient for the controlled release of drugs than those with PMAA segments. The release experiments at 37 °C and room temperature show comparable kinetic profiles, whereas drug release rates are significantly reduced in aqueous solutions with pH 7.4. The dependence of the release behavior on the drug concentration follows first-order kinetics . The presence of PCL segment(s) ensures the biodegradability and biocompatibility of the resulting self-assemblies, while P(M)AA segments are expected to influence the bioadhesion of particles suggesting their effectiveness as oral or aerosol micellar systems[19].

Acknowledgments

This work was financially supported by the European Social Fund, Operational Programme Human Capital, Project UDA-POKL.04.01.01-00-114/09-00 (K.B.). F.D.P. acknowledges the Belgian Program on Interuniversity Attraction Poles initiated by the Belgian State, the Prime Minister's office (P7/05) and the European Science Foundation – Precision Polymer Materials (P2M) program for financial support.

Received:

Revised:

Published online:

Keywords

micelle, drug-loading, block copolymers, poly(ε-caprolactone), poly[(meth)acrylic acid], indomethacin, quercetin.

References

[1] A. Blanazs, S. P. Armes, A. J. Ryan, *Macromol. Rapid Commun.* **2009**, *30*, 267.

[2] Z. Ge, S. Liu, *Macromol. Rapid Commun.* **2009**, *30*, 1523.

[3] X. J. Loh, B. J. H. Yee, F. S. Chia, *J. Biomed. Mater. Res. Part A* **2012**, *100A*, 2686.

[4] F. Ungaro, C. Conte, L. Ostacolo, G. Maglio, A. Barbieri, C. Arra, G. Misso, A. Abbruzzese, M. Caraglia, F. Quaglia, *Nanomedicine: Nanotechnology, Biology, and Medicine* **2012**, *8*, 637.

[5] P. Alonso-Cristobal, M. Laurenti, F. J. Sanchez-Muniz, E. López-Cabarcos, J. Rubio-Retama, *Polymer* **2012**, *53*, 4569.

[6] X. Huang, Y. Xiao, M. Lang, *Carbohydrate Polymers* **2012**, *87*, 790.

[7] S. Y Kim, Y. M. Lee, *Biomaterials* **2001**, *22*, 1697.

[8] J. C. Ha, S. Y. Kim, Y. M. Lee, *J. Controlled Release* **1999**, *62*, 381.

[9] V. Kumar, R. K. Prud'homme, *J. Pharm. Sci.* **2008**, *97*, 4904.

[10] S. Y. Kim, I. G. Shin, Y. M. Lee, Ch. S. Cho, Y. K. Sung, *J. Controlled Release* **1998**, *51*, 13.

[11] V. San Miguel, A. J. Limer, D. M. Haddleton, F. Catalina, C. Peinado, *Eur. Polym. J.* **2008**, *44*, 3853.

[12] R. Savic, T. Azzam, A. Eisenberg, D. Maysinger, *Langmuir* **2006**, *22*, 3570.

[13] H. M. Aliabadi, D. R. Brocks, A. Lavasanifar, *Biomaterials* **2005**, *26*, 7251.

[14] B. S. Lele, J.-C. Leroux, *Polymer* **2002**, *43*, 5595.

[15] Ch. Allen, J. Han, Y. Yu, D. Maysinger, A. Eisenberg, *J. Control. Release* **2000**, *63*, 275.

[16] J. Ch. Ha, S. Y. Kim, Y. M. Lee, *J. Control. Release* **1999**, *62*, 381–392; **2000**, *65*, 345.

[17] A. L. Glover, S. M. Nikles, J. A. Nikles, Ch. S. Brazel, D. E. Nikles, *Langmuir* **2012**, *28*, 10653.

[18] X. Huang, Y. Xiao, M. Lang, *J. Colloid and Interface Sci.* **2011**, *364*, 92.

[19] C. Allen, D. Maysinger, A. Eisenberg, *Colloids and Surfaces B : Biointerfaces* **1999**, *16*, 3.

[20] W.-H. Chen, M.-Y. Hua, R.-S. Lee, *J. Appl. Polym. Sci.* **2012**, *125*, 2902.

[21] L. Ould-Ouali, A. Ariën, J. Rosenblatt, A. Nathan, P. Twaddle, T. Matalenas, M. Borgia, S. Arnold, D. Leroy, M. Dinguizli, L. Rouxhet, M. Brewster, V. Preat, *Pharm. Res.* **2004**, *21*, 1581.

[22] S. Y. Kim, Y. M. Lee, H. J.; Shin, J. S. Kang, *Biomaterials* **2001**, *22*, 2049.

[23] I. G. Shin, S. Y. Kim, Y. M. Lee, Ch. S. Cho, Y. K. Sung, *J. Controlled Release* **1998**, *51*, 1.

[24] F. Wang, T. K. Bronich, A. V. Kabanov, R. D. Rauh, J. Roovers, *Bioconjugate Chem.* 2005, 16, 397.

[25] M. Materska, *Pol. J. Food Nutr. Sci.* **2008**, *58*, 407.

[26] X. Yang, B. Yhu, T. Dong, P. Pan, X. Shuai, Y. Inoue, *Macromol. Biosci.* **2008**, *8*, 1116.

[27] Q. Zhang, E. E. Remsen, K. L. Wooley, *J. Am. Chem. Soc.* 2000, 122, 3642.

[28] P.-F. Gou, W.-P. Zhu, N. Zhu, Z.-Q. Shen, *J. Polym. Sci.: Part A: Polym. Chem.* **2009**, *47*, 2905.

[29] K. M. Stridsberg, M. Ryner, A. C. Albertsson, *Adv. Polym. Sci.* **2000**, *157*, 41.

[30] D. Neugebauer, K. Bury, P. Maksym-Bębenek, T. Biela, *Polym. Int.*, DOI 10.1002/pi.4360.

[31] C. Burguiere, S. Pascual, C. Bui, J.-P. Vairon, B. Charleux, K. A. Davis, K. Matyjaszewski, I. Betremieux, *Macromolecules* **2001**, *34*, 4439.

[32] H. Mori, D. Ch. Seng, H. Lechner, M. Zhang, A. H. E. Mueller, *Macromolecules* **2002**, *35*, 9270.

[33] S. Hou, E. L. Chaikof, D. Taton, Y. Gnanou, *Macromolecules* **2003**, *36*, 3874.

[34] S. Balayssac, V. Gilard, M.-A. Delsuc, M. Malet-Martino, *Spectroscopy Europe* **2009**, *21*, 10.

[35] J. Rodrıguez-Hernandez, F. Checot, Y. Gnanou, S. Lecommandoux, *Prog. Polym. Sci.* **2005**, *30*, 691.

[36] S. Strandman, S. Hietala, V. Aseyev, B. Koli, S. J. Butcher, H. Tenhu, *Polymer* **2006**, *47*, 6524.

[37] A. N. Kuskov, A. A. Voskresenskaya, A. V. Goryachaya, A. A. Artyukhov, M. I. Shtilman, A. M. Tsatsakis, *J. Mater. Sci.: Mater. Med.* **2010**, *21*, 1521.

[38] D. W. Miller, A. V. Kabanov, *Colloids and Surfaces B : Biointerfaces* **1999**, *16*, 321.

[39] The DrugBank Open Data Drug & Drug Target Database http://www.drugbank.ca/

[40] H. M. Maswadeh, M. H. Semreen, A. A. Abdulhalim, *Acta Poloniae Pharmaceutica - Drug Research,* **2006**, *63*, 63.

[41] H. Banu, M. R. Sahariar, M. S. B. Sayeed, I. Dewan, S. M. Ashraful Islam, *J. Chem. Pharm. Res*. **2011**, *3(6)*, 348.

[42] G. S. Banker, C. T. Rhodes, *Modern pharmaceutics*, Marcel Dekker Inc., New York, USA **2002**.

[43] P. L. Soo, L. Luo, D. Maysinger, A. Eisenberg, *Langmuir* **2002**, *18*, 9996.

Schemes

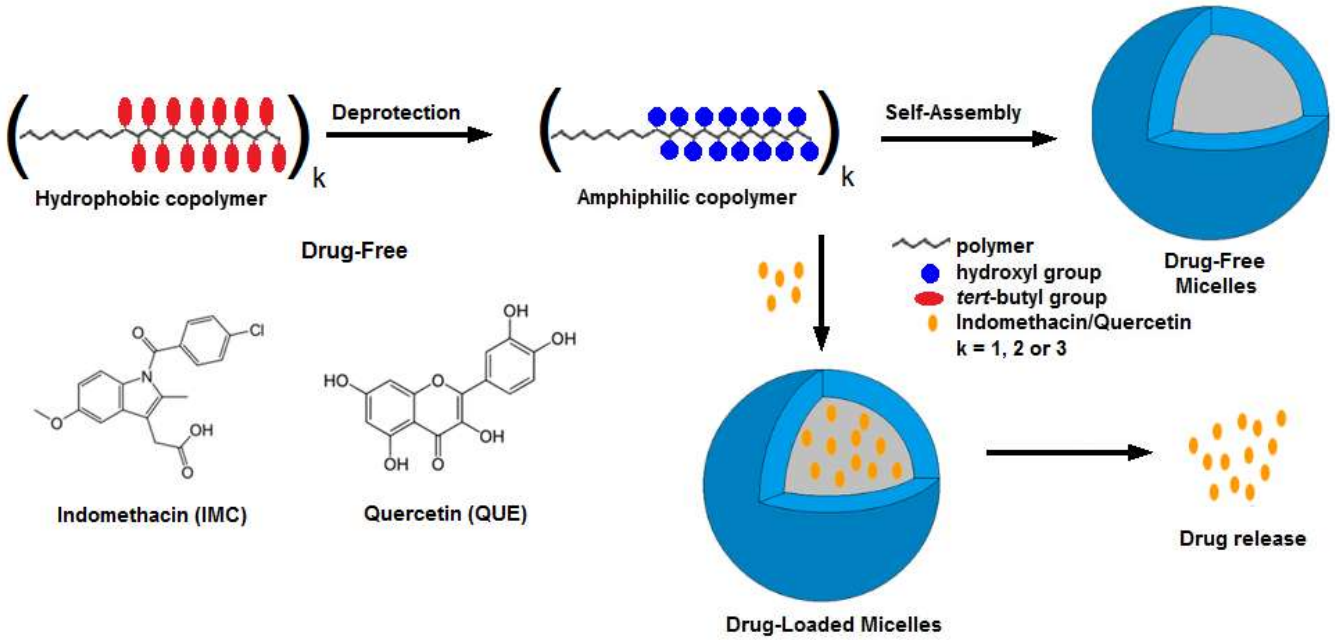

Scheme 1. Schematic illustration of self-assembly of amphiphilic block copolymers.

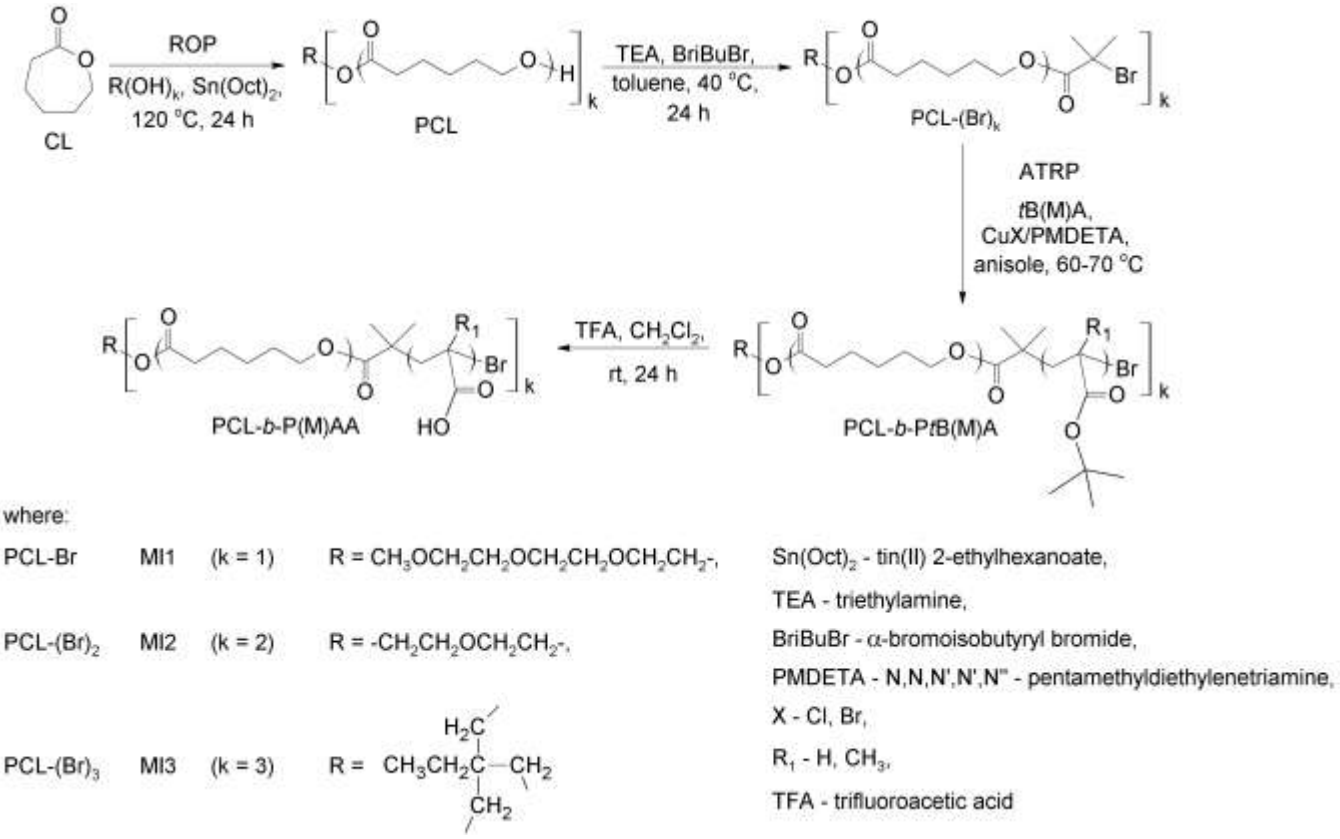

where:

PCL-Br	MI1	(k = 1)	R = $CH_3OCH_2CH_2OCH_2CH_2OCH_2CH_2$-,	$Sn(Oct)_2$ - tin(II) 2-ethylhexanoate,
$PCL-(Br)_2$	MI2	(k = 2)	R = $-CH_2CH_2OCH_2CH_2$-,	TEA - triethylamine,
$PCL-(Br)_3$	MI3	(k = 3)	R =	BriBuBr - α-bromoisobutyryl bromide,
				PMDETA - N,N,N',N'',N''' - pentamethyldiethylenetriamine,
				X - Cl, Br,
				R_1 - H, CH_3,
				TFA - trifluoroacetic acid

Scheme 2. Transformation of hydrophobic to amphiphilic block copolymers based on PCL.

Figures

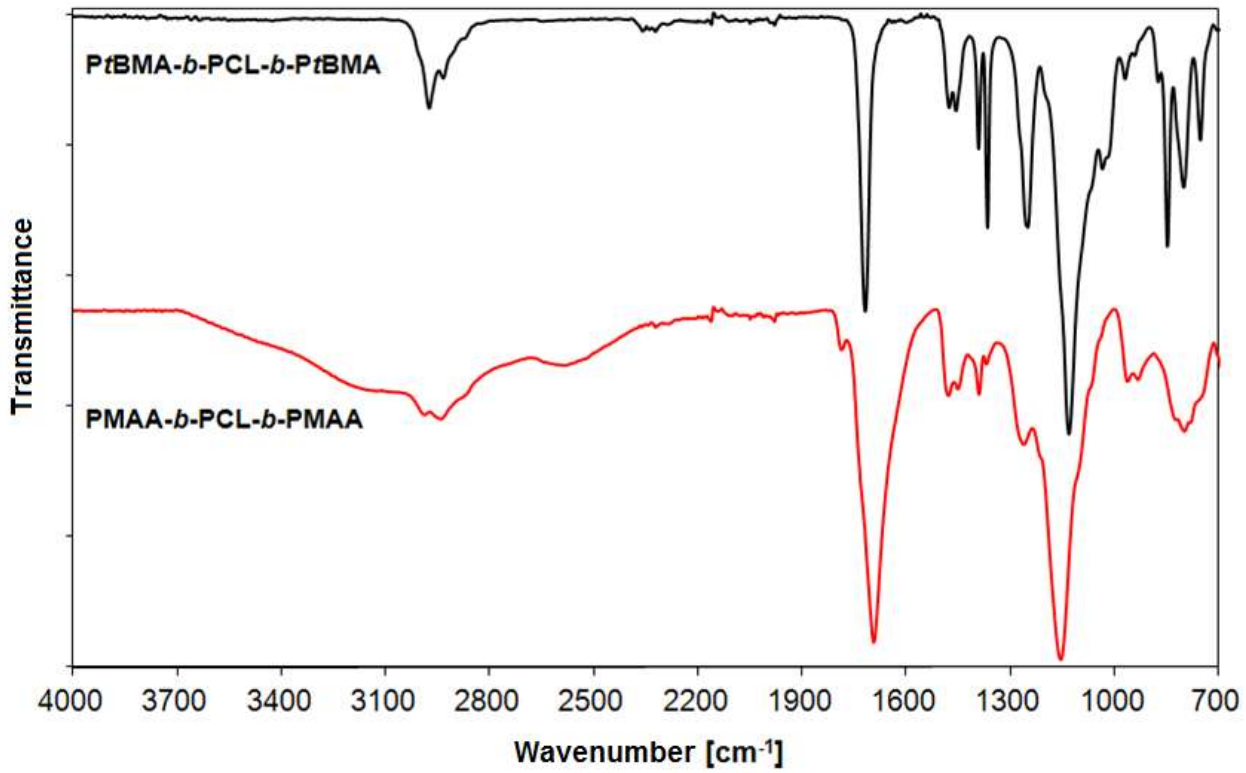

Figure 1. HATR-FTIR spectra of triblock copolymer **III** before and after deprotection of acidic groups.

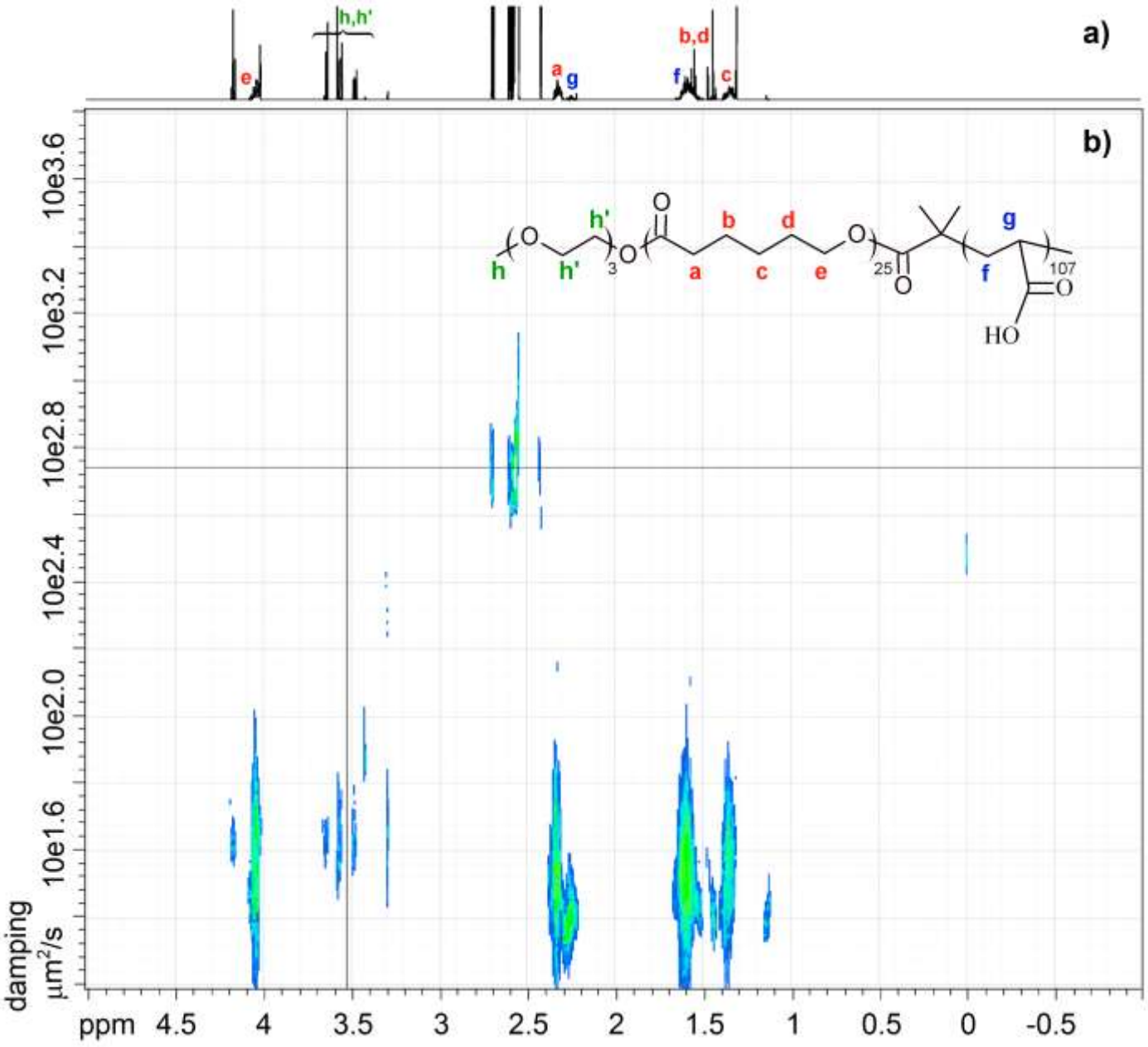

Figure 2. ^{1}H NMR (a) and Contour Plot DOSY ^{1}H NMR spectrum (b) of AB block copolymer (**VI**) in DMSO-d_6.

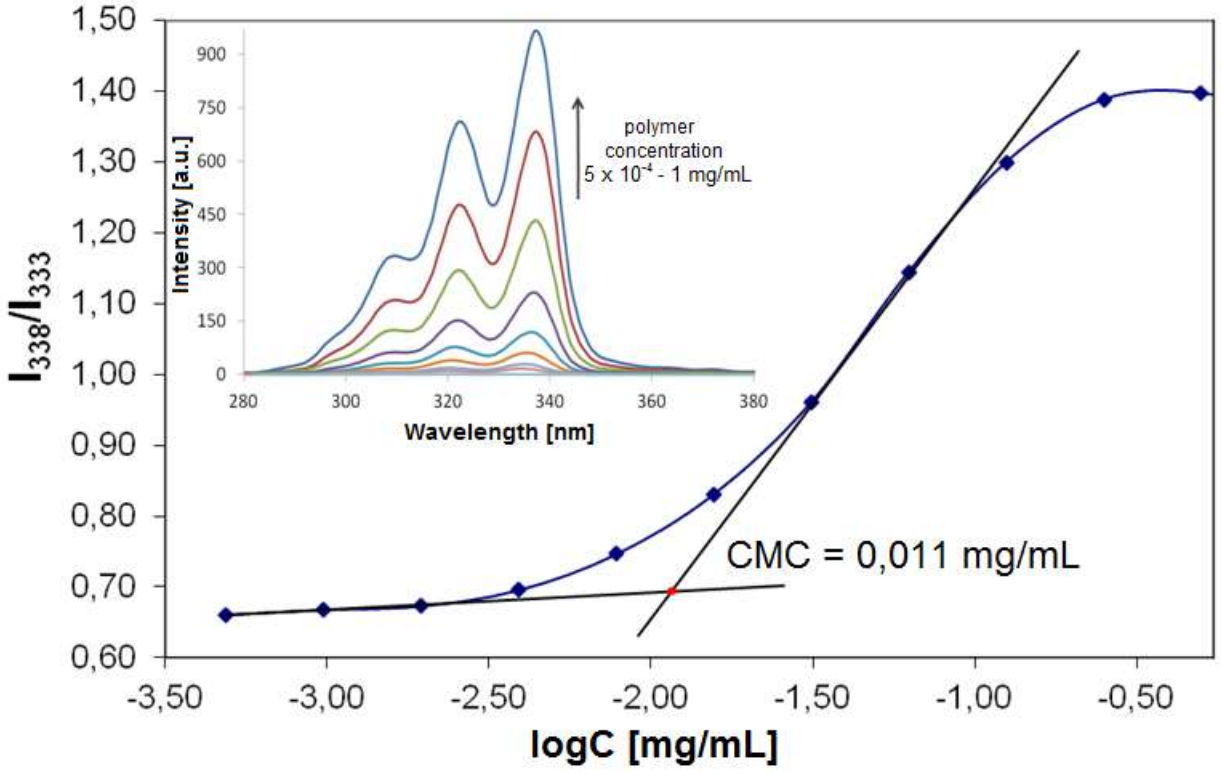

Figure 3. Plot of the intensity ratio I_{338}/I_{333} from pyrene excitation spectra (at λ_{em} = 390 nm) vs. nanoparticle concentration (logC) for BAB copolymer (**III**). The inset shows the excitation spectra of pyrene at a constant λ_{em} = 390 nm as a function of copolymer concentration (5 x 10^{-4} – 1 mg/ml).

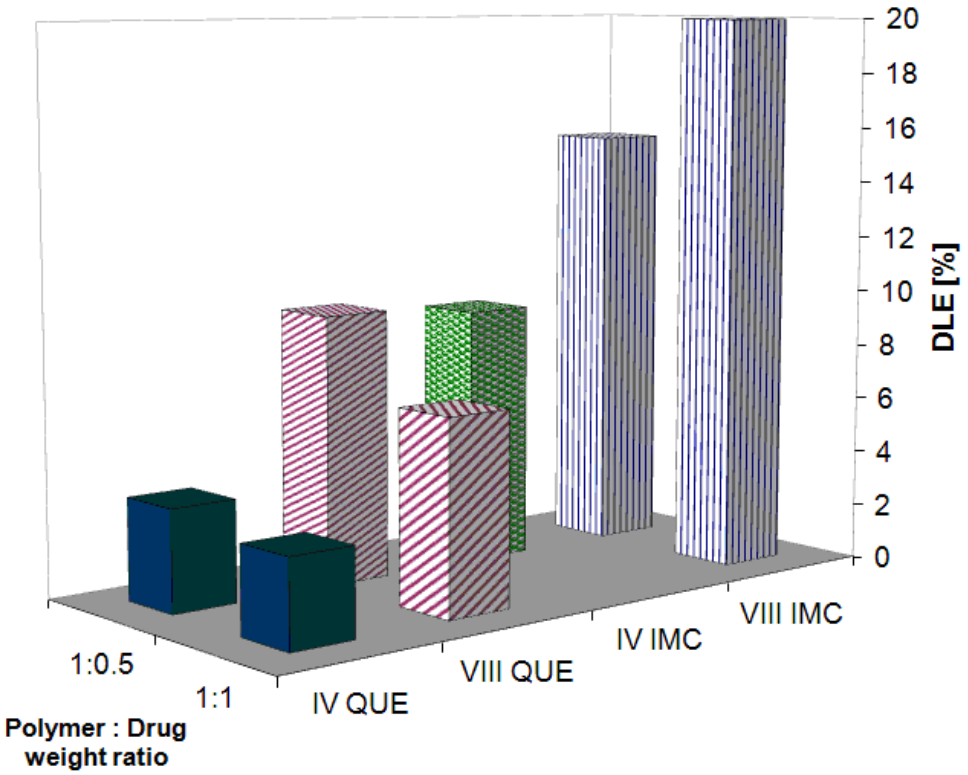

Figure 4. Effect of weight ratio of amphiphilic copolymer to drug on drug loading efficiency of polymeric nanoparticles.

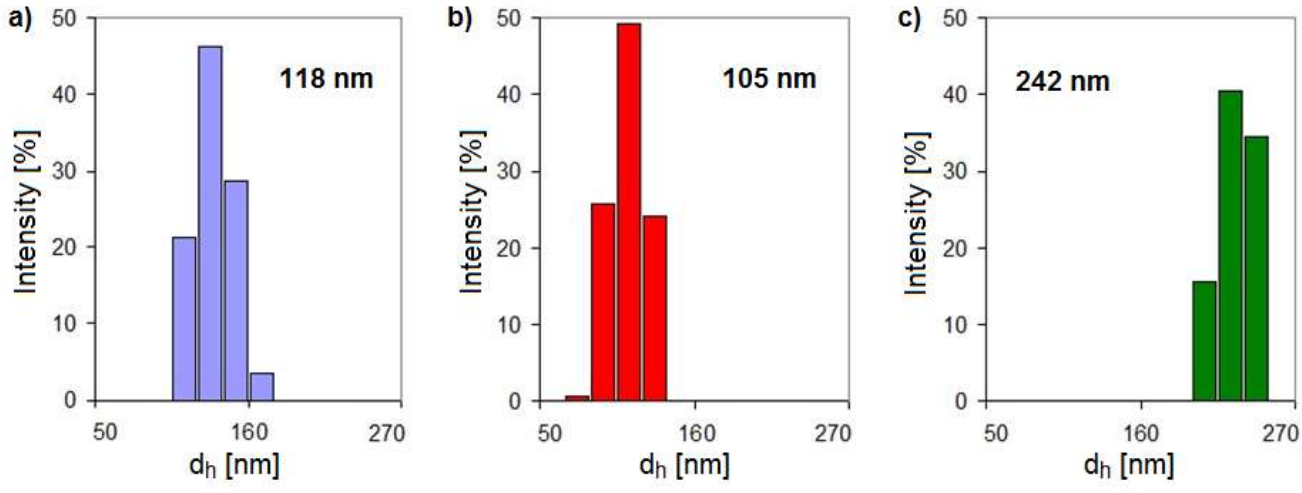

Figure 5. Size distribution profiles (by intensity) of nanoparticles based on AB_3 copolymer (**IV**) by DLS measurements in aqueous solutions of a) drug-free at 25 °C, b) drug-free at 37 °C, and c) IMC-loaded at 37 °C.

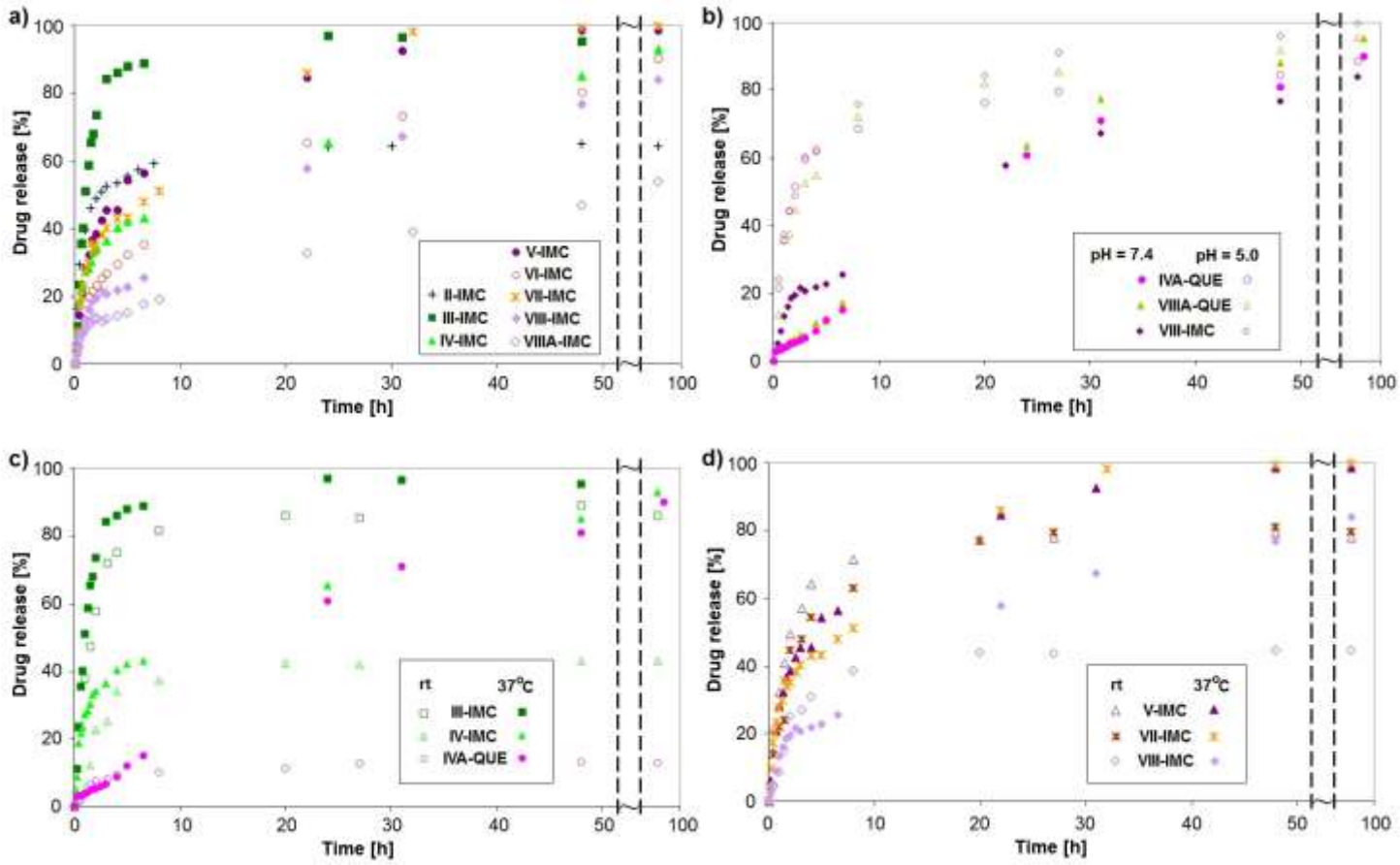

Figure 6. Drug release profiles from IMC-loaded nanoparticles based on copolymers with different topologies (pH = 7.4 at 37 °C) (a), $(AB)_3$ based particles at different pH (37 °C) (b), PCL/PMAA based particles (c), and PCL/PAA particles (d) at different temperature (pH = 7.4).

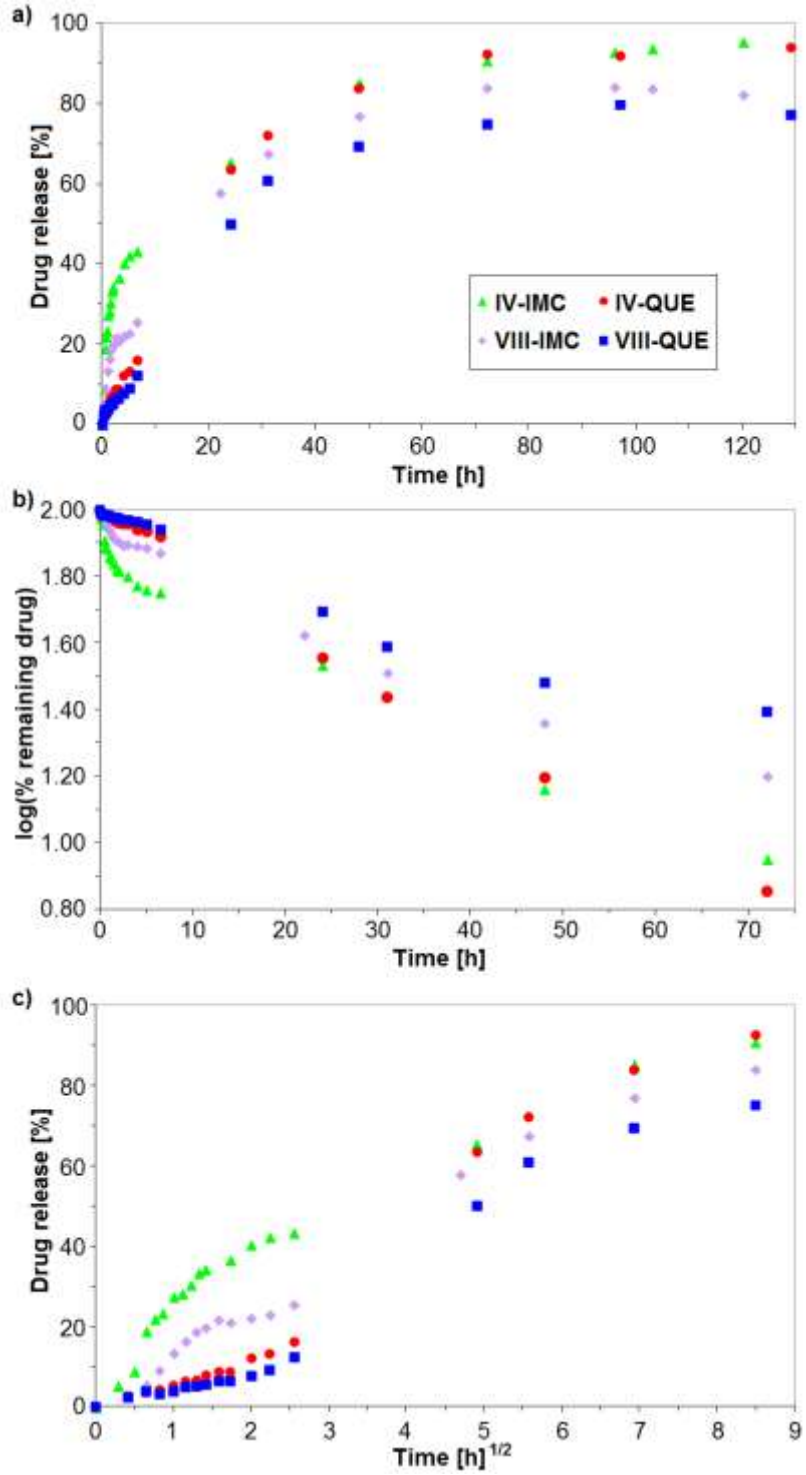

Figure 7. The kinetics of drug release in PBS with pH = 7.4 at 37 °C from nanoparticles loaded with IMC and QUE a) zero-order plot of percentage of drug released in time, b) a linear plot of log (% remaining drug) vs. time for the release data accordance with the first-order equation, and c) a linear plot of % of released drug vs. square root of time for the release data in accordance with the Higuchi square root model.

Tables

Table 1. Properties of the amphiphilic block copolymers used for micellization.

No	Polymer structure[a)]	DP_{CL}	$DP_{(M)AA}$	$m_{(M)AA}$[b)]	$F_{hydrophil.}$ [mol%]
		PCL-*b*-PMAA			
I	AB	25	70	70	74
II	AB	25	89	89	78
III	BAB	20	257	128	93
IV	$(AB)_3$	10	181	60	95
		PCL-*b*-PAA			
V	AB	25	38	38	60
VI	AB	25	107	107	81
VII	BAB	20	162	81	89
VIII	$(AB)_3$	10	208	69	95

[a)] A = PCL; DP_{CL} = 25 for copolymers with AB structure, DP_{CL} = 20 for BAB copolymers, DP_{CL} = 10 for $(AB)_3$ copolymers; [b)] number of units in one poly(meth)acrylic block

Table 2. CAC, drug loading and drug entrapment efficiencies for polymeric nanoparticles.

No	CAC [mg/ml]	IMC		QUE	
		DLE [%]	DEE [%]	DLE [%]	DEE [%]
I	0.009	56.8	76.7	-	-
II	0.018	18.8	24.2	-	-
III	0.012	29.2	21.4	-	-
IV	0.067	9.3	12.8	3.7	5.1
IVA		-	-	3.2	2.1
V	0.006	13.4	11.5	-	-
VI	0.009	10.0	9.0	-	-
VII	0.013	17.2	22.6	-	-
VIII	0.122	15.4	17.1	9.7	16.3
VIIIA		20.0	10.4	6.9	7.2

polymer:drug = 1:0.5 with exception of **IVA** and **VIIIA** (1:1), dash "-" means not determined.

Table 3. Drug-free and drug-loaded particle's sizes.

No	Mean particle size at 25 °C [nm]						Mean particle size at 37 °C [nm]					
	Drug free	**PDI**	**IMC load.**	**PDI**	**QUE load.**	**PDI**	**Drug free**	**PDI**	**IMC load.**	**PDI**	**QUE load.**	**PDI**
I	66	0.488	81	0.459	-	-	63	0.477	-	-	-	-
II	90	0.374	155	0.462	-	-	88	0.425	-	-	-	-
III	74	0.470	-	-	-	-	69	0.508	-	-	-	-
IV	118	0.573	235	0.131	201	0.243	105	0.601	242	0.178	206	0.263
IVA			-	-	161	0.235			-	-	162	0.251
V	50	0.133	175	0.472	-	-	53	0.250	172	0.548	-	-
VI	153	0.235	71	0.251	-	-	147	0.260	72	0.260	-	-
VII	115	0.429	224	0.227	-	-	124	0.480	205	0.236	-	-
VIII	120	0.459	233	0.231	231	0.132	133	0.612	226	0.217	231	0.133
VIIIA			245	0.266	-	-			236	0.292	-	-

polymer:drug = 1:0.5 with exception of **IVA** and **VIIIA** (1:1), dash "-" means not determined.

Table 4. The percentage of drug released at different pH and temperature.

No	IMC release [%]			QUE release [%]		
	pH = 5	**pH = 7.4**	**pH = 7.4**	**pH = 5**	**pH = 7.4**	pH = 7.4
	37°C		**rt**	**37 °C**		rt
I	-	28.5	-	-	-	-
II	-	58.6	-	-	-	-
III	-	96.3	-	-	-	86.2
IV	-	95.7	43.2	-	94.3	-
IVA	-	-	-	86.9	90.6	13.1
V	93.5	99.9	78.1	-	-	-
VI	-	89.3	-	-	-	-
VII	-	99.6	79.7	-	-	-
VIII	99.9	82.3	44.7	-	77.5	-
VIIIA	-	53.1	-	95.8	98.5	-

polymer:drug = 1:0.5 with exception of **IVA** and **VIIIA** (1:1), rt – room temperature, dash "-" means not determined.

K. Bury, F. Du Prez, D. Neugebauer*

Self-assembling linear and star shaped poly(ε-caprolactone)/poly[(meth)acrylic acid] block copolymers as carriers of indomethacin and quercetin

An investigation of nanoparticles prepared from linear AB, BAB and star-shaped $(AB)_3$ block copolymers based on poly(ε-caprolactone) and poly(meth)acrylic acid is performed to determine the influence of the polymer's topology and composition on the drug loading and release properties. The self-assemblies have been tested as nanocarriers of indomethacin and quercetin, which can be applied in controlled delivery systems.

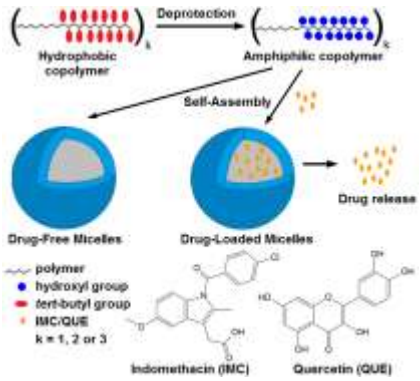

ToC figure